

Low energy kaon-nuclei interaction studies at DAΦNE

Kristian Piscicchia^{1,2,*}, *Michael Cargnelli*³, *Raffaele Del Grande*^{4,2}, *Laura Fabbietti*^{5,4}, *Johann Marton*³, *Pawel Moskal*⁶, *Alessandro Scordo*², *Diana Sirghi*², *Magdalena Skurzok*^{2,6}, *Oton Vazquez Doce*², *Slavomir Wycech*⁷, *Johann Zmeskal*³, *Paolo Branchini*⁸, *Eryk Czerwinski*⁶, *Veronica De Leo*^{9,10}, *Erika De Lucia*², *Alessandro Di Cicco*^{11,8}, *Eleonora Diociaiuti*², *Paolo Fermani*², *Salvatore Fiore*^{12,10}, *Matteo Martini*^{2,13}, *Elena Perez Del Rio*^{9,10}, *Andrea Selce*^{11,8}, *Michal Silarski*⁶, and *Catalina Curceanu*²

¹Centro Ricerche Enrico Fermi - Museo Storico della Fisica e Centro Studi e Ricerche “Enrico Fermi”, 00184 Rome, Italy

²INFN - Laboratori Nazionali di Frascati, 00044 Frascati, Italy

³Stefan-Meyer-Institut für Subatomare Physik, 1030 Wien, Austria

⁴Physik Department E12, Technische Universität München, 85748 Garching, Germany

⁵Excellence Cluster “Origin and Structure of the Universe”, 85748 Garching, Germany

⁶Institute of Physics, Jagiellonian University, 30-348 Cracow, Poland

⁷National Centre for Nuclear Research, 02-093 Warsaw, Poland

⁸INFN Sezione di Roma Tre, Roma, Italy

⁹Dipartimento di Fisica dell’Università “Sapienza”, Roma, Italy

¹⁰INFN Sezione di Roma, Roma, Italy

¹¹Dipartimento di Matematica e Fisica dell’Università “Roma Tre”, Roma, Italy

¹²ENEA, Department of Fusion and Technology for Nuclear Safety and Security, Frascati (RM), Italy

¹³Dipartimento di Scienze e Tecnologie applicate, Università “Guglielmo Marconi”, Roma, Italy

Abstract. The aim of the AMADEUS experiment is to investigate the low-energy antikaon interaction with nucleons and nuclei, exploiting the unique low-momentum beam of kaons produced by the DAΦNE collider at LNF-INFN, to constrain hadronic nuclear physics models in the strangeness -1 sector.

As a first step the data collected in 2004/2005 by the KLOE collaboration, consisting in a complex of K^- absorptions in H, ^4He , ^9Be and ^{12}C , was analyzed, leading to the first invariant mass spectroscopic study with very low momentum (about 100 MeV) in-flight K^- captures. A dedicated pure Carbon target was also implemented in the central region of the KLOE detector, providing a high statistic reference sample of pure at-rest K^- nuclear interaction. The first measurement of the non-resonant transition amplitude $|T_{K^-n \rightarrow \Lambda \pi^-}|$ at $\sqrt{s} = 33$ MeV below the $\bar{K}N$ threshold is presented, in relation with the $\Lambda(1405)$ properties studies.

1 INTRODUCTION

A specimen of the analyses which are being performed by the AMADEUS collaboration will be described. We will be in particular concerned on the investigation of the resonant and non-resonant transition amplitudes, below the $\bar{K}N$ threshold. These studies take advantage of

*e-mail: kristian.piscicchia@creef.it

the unique low momentum kaons beam produced by the DAΦNE collider [1] at the Frascati National Laboratory of INFN. At-rest and low-momentum in-flight ($p_K \sim 127$ MeV/c) K^- mesons captures on ^4He and ^{12}C nuclear targets are exploited. The study is aimed to provide constraints to the non-perturbative strong interaction models in the strangeness sector.

Quantitative information on the yield and the spectral shape of the non-resonant antikaon-nucleon absorption transition amplitude, below the $\bar{K}N$ threshold, giving rise to a hyperon-pion final state, is a useful reference to extract the $\Lambda(1405)$ properties and to disentangle this state from the competing non-resonant $(\Sigma\pi)^0$ production in $\bar{K}N$ absorption experiments.

The antikaon-nucleon strong interaction is dominated by the emergence of the (1405) (isospin $I=0$) state below the $\bar{K}N$ threshold. Phenomenological potential models (see e.g. Refs. [2, 3]) interpret the (1405) as a pure $\bar{K}N$ bound state with a Binding Energy of about 27 MeV. According to chiral unitary models [4–10] the (1405) emerges from the interference of two poles, as a molecular meson-baryon state. A lower pole, with a mass of about 1390 MeV, is mainly coupled to the $\Sigma\pi$ decay channel, a higher mass pole, which is mainly coupled to the $\bar{K}N$ channel, is located around 1420 MeV (see also [11]). The shape of the measured $(\Sigma\pi)^0$ invariant mass distribution should thus depend on both the decay channel (as a consequence of the isospin interference term, which contributes with opposite sign to the $\Sigma^\pm\pi^\mp$ cross sections and vanishes for $\Sigma^0\pi^0$) and on the production channel. In this scenario $\bar{K}N$ absorption represents the golden channel for investigating the predicted high mass pole of the $\Lambda(1405)$. The experimental characterisation of the antikaon-nucleon amplitude below threshold is a good constraint for the chiral predictions (see e.g. [6, 12]) since the real and imaginary parts of the calculated transition amplitudes are strongly model dependent in the sub-threshold region both in $I=0$ and $I=1$.

The analysed data sample collected by the KLOE collaboration in 2004/2005 [13] permits investigating both at rest ($p_K \sim 0$) and in-flight low momentum K^- nuclear absorptions. In the case of interactions at-rest the underlying mechanism consists in the capture of the strange meson in a highly excited atomic state and a successive cascade to low-lying states, followed by the K^- nuclear capture. Besides the interactions at-rest, an important contribution from in-flight K^- nuclear captures was already characterised by the AMADEUS collaboration in previous works (see e.g. [14]). In this case the kaon crosses the electron cloud, and is directly absorbed by the nucleus. We will show that low-momentum kaon induced reactions in-flight can give important information on the $\Lambda(1405)$ high mass pole properties.

2 DATA SAMPLES

We are presently analyzing two complementary samples of data. The first one is represented by the data collected by the KLOE collaboration during the 2004/2005 data taking campaign, and corresponds to an integrated luminosity of about 1.74 fb^{-1} . In this case the KLOE detector is used as an active target, the hadronic interaction of negative kaons with the materials of the apparatus being investigated; in particular $K^-^9\text{Be}$ absorptions in the DAΦNE Beryllium thin cylindrical layer and the DAΦNE aluminated beryllium pipe, $K^-^{12}\text{C}$ and K^-^H absorptions in the KLOE Drift Chamber [15] (DC) inner wall (aluminated carbon fiber), $K^-^4\text{He}$ in the DC gas, filled with a mixture of Helium and Isobutane (in volume: 90% ^4He and 10% C_4H_{10}). This sample provides extremely rich experimental information, since it contains K^- hadronic captures both at-rest and in-flight.

A second dedicated measurement was performed in 2012, with a high purity carbon (graphite) target, which was installed between the beam pipe and the KLOE DC inner wall. Aim of the measurement was to collect a reference sample of pure K^- absorption at-rest in ^{12}C . The geometry of the target was optimized to maximize the kaon stopping power (techni-

cal details can be found in Ref. [14]). The total reconstructed integrated luminosity amounts to about 37 pb^{-1} .

The detailed event selection and particle identification procedure, for the analyses which is described in this work, is reported in Ref. [14].

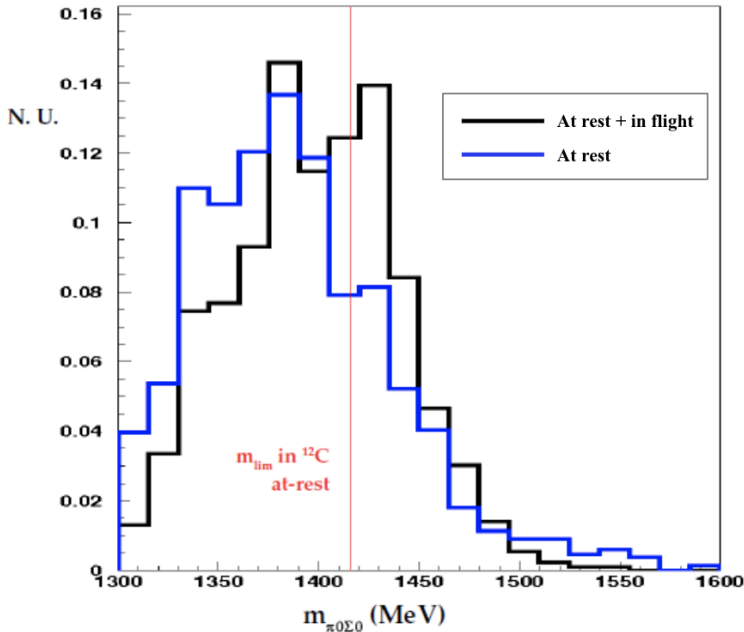


Figure 1. (Colour online.) $m_{\Sigma^0\pi^0}$ invariant mass distribution from K^- captures in the KLOE DC wall (black curve) and pure carbon graphite target (blue curve).

3 RESONANT AND NON RESONANT $\Sigma\pi$ TRANSITION AMPLITUDES BELOW THE $\bar{K}N$ THRESHOLD

The investigation of the $\Lambda(1405)$ properties in K^- induced reactions on light nuclear targets is strongly biased by the kinematic threshold, determined by the absorbing nucleon binding energy. For K^- captures at-rest on ^4He and ^{12}C the $m_{\Sigma\pi}$ invariant mass thresholds are about 1412 MeV and 1416 MeV respectively. The $m_{\Sigma\pi}$ range lying immediately below the $\bar{K}N$ threshold can be accessed, by exploiting the in-flight K^- capture process, taking advantage of the kaon kinetic energy contribution. For kaon momenta of 100 MeV/c the $m_{\Sigma\pi}$ threshold is shifted upwards by about 10 MeV, thus opening the mass window where the high mass pole of the $\Lambda(1405)$ is predicted.

In Fig. 1 (black distribution) the $\Sigma^0\pi^0$ invariant mass spectrum from K^- captures in the KLOE DC wall is shown [16]. $\Sigma^0\pi^0$ represents the best signature of the $\Lambda(1405)$ resonance, since it does not contain isospin $I = 1$ background. The $m_{\Sigma^0\pi^0}$ spectrum is compared with the corresponding distribution of K^- captures at-rest in the pure Carbon target (fig. 1 blue distribution). The blue and the black distributions are normalised to unity. In fig. 1 the red line indicates the energy threshold corresponding to K^- absorption in ^{12}C at-rest. A rich sample of in-flight $K^-^{12}\text{C}$ captures can be identified above the red line. The next steps of the data analysis, presently ongoing, consist in the subtraction of the non-resonant $\Sigma^0\pi^0$ formation

contribution, which is due to the K^- absorption on hydrogen, contained in the carbon fibre, and in a comparison of the obtained spectrum with models of $\Lambda(1405)$ production in K^- captures in-flight on ^{12}C .

The real and imaginary parts of the non-resonant coupled channels $K^-n \rightarrow \Lambda\pi/\Sigma\pi$ scattering amplitudes, were calculated on the basis of several chiral SU(3) meson-baryon coupled channels interaction models (we will use the following notation: Barcelona (BCN) [6], Kyoto-Munich (KM) [7], Prague (P) [8], Murcia (M1 and M2) [9], Bonn (B2 and B4) [10], see also Refs. [17, 18]). The amplitudes values strongly differ in the $\bar{K}N$ sub-threshold region depending on the adopted model.

In order to pin down the model to be adopted for the description of the observed $\Sigma^0\pi^0$ spectra, the $K^-n \rightarrow \Lambda\pi^-$ transition was measured by exploiting K^-n single nucleon absorptions in ^4He . Since the $\Sigma^-(1385)$ (isospin $I = 1$) resonance is well known, the corresponding non-resonant transition amplitude ($|T_{K^-n \rightarrow \Lambda\pi^-}|$) can be extracted, and used to test the chiral predictions below threshold. The details of the particle identification and event selection are given in Ref. [12]. The contribution of the Σ particle conversion events, to the measured sample, was minimised by selecting, in the p_{π^-} vs p_{Λ} scatterplot, the phase space region which is populated by the correlated direct $\Lambda\pi^-$ production. The phase space cut was optimised based on MC simulations (performed with the standard KLOE GEANT digitization (GEANFI [19])), according to the calculations reported in [20].

In order to extract the ratio of the resonant over non-resonant $\Lambda\pi^-$ production, the measured $p_{\Lambda\pi^-}$, $m_{\Lambda\pi^-}$ and $\cos(\theta_{\Lambda\pi^-})$ (total hyperon-pion momentum, invariant mass and the angle between the Λ and π momenta) distributions were fitted. The main background is represented by the contribution of $K^-^{12}\text{C}$ absorptions as a consequence of the presence of Isobutane molecules in the DC gas. In order to account for this contribution an experimental sample of $K^-^{12}\text{C}$ absorptions is used in the global fit. The carbon sample is obtained by selecting kaons interactions in the DC entrance wall, adopting the same criteria as for the gas sample. The modulus of the amplitude of the non-resonant processes, the ratio of the resonant to non-resonant processes, the modulus of the amplitude of the conversions and the contribution of the K^- captures on Carbon are considered as free parameters in the fit.

The results of the fit are summarised in Table I. (In Ref [12] the corresponding fit is shown in Fig. 3). The systematic errors are estimated by varying independently the selection cuts such as to increase or decrease the $\Lambda\pi^-$ statistics by 15% with respect to the optimized selection. The chi-square of the fit is $\chi^2/ndf = 151/148$. The ratio ($\frac{\text{RES-if}}{\text{NR-if}}$) for the $\Lambda\pi^-$ production in-flight is found to be smaller than the corresponding ratio at-rest. This is not surprising as the K^-n interaction in-flight occurs about $\sqrt{s} = 20$ MeV below the $\bar{K}N$ threshold; the corresponding reaction at-rest occurs about $\sqrt{s} = 33$ MeV below the threshold (see Ref. [20]), nearer to the resonance which lays about 49 MeV below the $\bar{K}N$ threshold. The systematic uncertainty on the resonant to non-resonant ratio for the in-flight reactions, prevents from extracting the modulus of the non-resonant transition amplitude in-flight. The corresponding transition amplitude modulus at-rest, extracted by comparing Eq. (14) and Eq. (20) in Ref. [20] with the experimental result ($\frac{\text{RES-ar}}{\text{NR-ar}}$) is:

$$|T_{K^-n \rightarrow \Lambda\pi^-}| = (0.334 \pm 0.018 \text{ stat}_{-0.058}^{+0.034} \text{ syst}) \text{ fm}. \quad (1)$$

4 DISCUSSION

In this work a summary of the measurement of the isospin $I = 1$ non-resonant transition amplitude $|T_{K^-n \rightarrow \Lambda\pi^-}|$ at $\sqrt{s} = 33$ MeV below the $\bar{K}N$ threshold is presented. The result of this analysis (with combined statistical and systematic errors) is shown in Fig. 2 and compared

Channels	Ratio/yield	σ_{stat}	σ_{syst}
RES-ar/NR-ar	0.39	± 0.04	$+0.18$ -0.07
RES-if/NR-if	0.23	± 0.03	$+0.23$ -0.22
NR-ar	12.0 %	$\pm 1.7 \%$	$+2.0 \%$ -2.8%
NR-if	19.2 %	$\pm 4.4 \%$	$+5.9 \%$ -3.3%
$\Sigma \rightarrow \Lambda$ conv.	2.2 %	$\pm 0.3 \%$	$+1.6 \%$ -0.8%
$K^{-12}\text{C}$ capture	57.0 %	$\pm 1.2 \%$	$+2.2 \%$ -3.2%

Table 1. Resonant to non-resonant ratios and amplitudes of the various channels extracted from the fit of the $\Lambda\pi^-$ sample. We indicate with RES and NR resonant and non-resonant processes respectively, the abbreviations ar and if are used for captures at-rest and in-flight. The statistical and systematic errors are also shown. See text for details.

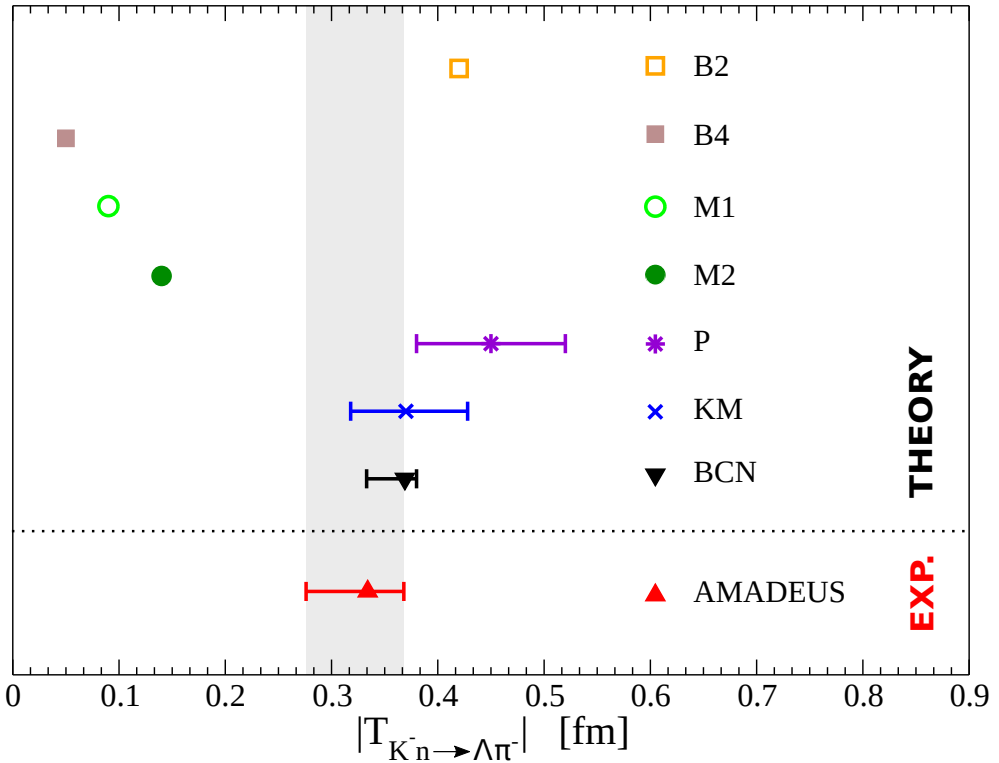


Figure 2. (Color online) Modulus of the non-resonant transition amplitude for the $K^-n \rightarrow \pi^-$ process obtained by AMADEUS in Ref. [20], compared with theoretical predictions: Barcelona (BCN) [6], Kyoto-Munich (KM) [7], Prague (P) [8], Murcia (M1 and M2) [9], Bonn (B2 and B4) [10].

with the theoretical predictions (BCN [6], KM [7], P [8], M1 and M2 [9], B2 and B4 [10]), re-scaled for the $K^-n \rightarrow \Sigma\pi$ transition probabilities. The presented result allows an extrapolation to the un-physical region and can be used to test models of S-wave interaction; moreover such extrapolation can be used to constrain the corresponding $(\Sigma\pi)^0$ non-resonant background for

the extraction of the $\Lambda(1405)$ properties in $\bar{K}N$ absorption experiments. In this direction an analogous, theoretical and experimental, analysis of the in medium K^-p absorption is ongoing.

ACKNOWLEDGMENTS

We acknowledge the KLOE/KLOE-2 Collaboration for their support and for having provided us with the data and the tools to perform the analysis presented in this paper. Part of this work was supported by Ministero degli Affari Esteri e della Cooperazione Internazionale, Direzione Generale per la Promozione del Sistema Paese (MAECI), Strange Matter project PRG00892; EU STRONG-2020 project (grant agreement No 824093); Polish National Science Center through grant No. UMO-2016/21/D/ST2/01155.

References

- [1] A. Gallo *et al.*, Conf. Proc. C **060626**, 604 (2006)
- [2] L. R. Staronski and S. Wycech, Journal of Physics G: Nuclear Physics, **13**, no. 11, 1361 (1987).
- [3] Y. Akaishi and T. Yamazaki, Phys. Rev. C **65**, 044005 (2002).
- [4] J. A. Oller and U. G. Meissner, Phys. Lett. B **500**, 263-272 (2001).
- [5] D. Jido, J. A. Oller, E. Oset, A. Ramos and U. G. Meissner, Nucl. Phys. A **725**, 181-200 (2003).
- [6] A. Feijoo, V. Magas and A. Ramos, Phys. Rev. C **99**, no.3, 035211 (2019).
- [7] Y. Ikeda, T. Hyodo and W. Weise, Nucl. Phys. A **881**, 98 (2012).
- [8] A. Cieplý and J. Smejkal, Nucl. Phys. A **881**, 115 (2012).
- [9] Z. H. Guo and J. A. Oller, Phys. Rev. C **87**, 035202 (2013).
- [10] M. Mai and U. G. Meißner, Eur. Phys. J. A **51**, 30 (2015).
- [11] S. Acharya *et al.* [ALICE], Phys. Rev. Lett. **124**, no.9, 092301 (2020).
- [12] K. Piscicchia *et al.*, Phys. Lett. B **782**, 339 (2018)
- [13] F. Bossi, E. De Lucia, J. Lee-Franzini, S. Miscetti, M. Palutan [KLOE Collaboration], Riv. Nuovo Cim. **31**, 531 (2008)
- [14] C. Curceanu *et al.*, Acta Phys. Polon. B **46**, 203 (2015)
- [15] M. Adinolfi *et al.*, Nucl. Instrum. Meth. A **488**, 51 (2002)
- [16] K. Piscicchia, PhD thesis (2013), Università degli Studi di Roma Tre, <http://www.infn.it/thesis/PDF/getfile.php?filename=7097-Piscicchia-dottorato.pdf>
- [17] J. Hrtankova and J. Mares, Phys. Rev. C **96**, 015205 (2017)
- [18] A. Cieplý *et al.*, Nucl. Phys. A **954**, 17 (2016)
- [19] F. Ambrosino *et al.*, Nucl. Instrum. Meth. A **534**, 403 (2004)
- [20] K. Piscicchia, S. Wycech and C. Curceanu, Nucl. Phys. A **954**, 75 (2016)